

Article

Effect of Aluminide Coating Thickness on High-Temperature Fatigue Response of MAR-M247 Nickel-Based Superalloy

Mateusz Kopec 

Institute of Fundamental Technological Research, Polish Academy of Sciences, ul. Pawińskiego 5B, 02-106 Warsaw, Poland; mkopec@ippt.pan.pl

Abstract: In this paper, 20 μm and 40 μm thick aluminide coatings were deposited on MAR-M247 nickel-based superalloy through the chemical vapor deposition (CVD) process in a hydrogen protective atmosphere for 4 h and 12 h, respectively, at a temperature of 1040 °C and an internal pressure of 150 mbar. The effect of aluminide coating thickness on the high-temperature performance of the MAR-M247 nickel-based superalloy was examined during a fatigue test at 900 °C. After high-temperature testing, the specimens were subjected to fractographic analysis to reveal the damage mechanisms. No significant effect of coating thickness was found since the material exhibited a similar service life throughout the fatigue test when subjected to the same stress amplitude. One should stress that the coating remained well adhered after specimen fracture, confirming its effectiveness in protecting the material against high-temperature oxidation.

Keywords: fatigue; aluminide coatings; nickel alloys; high-temperature performance

1. Introduction

The demand for materials that can withstand extreme conditions has steadily increased in modern industries, especially in the aerospace and power-generation sectors [1]. Nickel-based superalloys, such as MAR-M247, have emerged as essential materials for components operating at high temperatures due to their excellent mechanical properties, thermal stability, and resistance to creep and oxidation [2]. MAR-M247, a second-generation nickel-based superalloy, is primarily utilized in turbine blades, combustion chambers, and other critical engine parts where performance at temperatures exceeding 900 °C is mandatory. This superalloy is characterized by its complex microstructure, consisting of a gamma (γ) matrix reinforced with a significant volume fraction of gamma prime (γ') precipitates, as well as various carbides and solid-solution-strengthening elements such as aluminum, titanium, and tantalum [3]. These microstructural features provide MAR-M247 with the necessary strength and stability required for high-temperature applications. However, even with these inherent properties, the surface of MAR-M247 is susceptible to oxidation, hot corrosion, and thermal fatigue when exposed to harsh operational environments. To enhance the high-temperature performance and longevity of MAR-M247 components, protective surface coatings such as aluminide coatings are often employed [4].

Aluminide coatings are widely used to improve the oxidation resistance and thermal stability of nickel-based superalloys [5]. These coatings function by forming a diffusion layer on the substrate enriched with aluminum, which subsequently develops a protective alumina layer on the surface during high-temperature exposure. The formation of this stable oxide layer serves as a barrier against oxygen diffusion and aggressive environmental attack, significantly improving the material's resistance to oxidation and hot corrosion [1,4]. Aluminide coatings can be deposited through various techniques, including pack cementation [6,7], chemical vapor deposition (CVD) [2,8], and slurry methods [9,10], each allowing for control over the coating's composition and thickness. The thickness of the aluminide coating is a crucial parameter that influences the protective capability



Citation: Kopec, M. Effect of Aluminide Coating Thickness on High-Temperature Fatigue Response of MAR-M247 Nickel-Based Superalloy. *Coatings* **2024**, *14*, 1072. <https://doi.org/10.3390/coatings14081072>

Academic Editor: Cecilia Bartuli

Received: 5 August 2024

Revised: 15 August 2024

Accepted: 20 August 2024

Published: 21 August 2024



Copyright: © 2024 by the author. Licensee MDPI, Basel, Switzerland. This article is an open access article distributed under the terms and conditions of the Creative Commons Attribution (CC BY) license (<https://creativecommons.org/licenses/by/4.0/>).

and mechanical performance of the coated superalloy [11]. While thicker coatings might offer enhanced oxidation resistance due to a more substantial alumina layer, they can also introduce detrimental effects such as increased thermal stress, potential spallation, and changes in the load-bearing capacity of the component. Conversely, thinner coatings may not provide sufficient protection against oxidation and other forms of degradation, leading to the premature failure of the superalloy substrate [12].

Understanding the impact of aluminide coating thickness on the high-temperature performance of MAR-M247 is essential for optimizing the protective capabilities of these coatings. This understanding involves a comprehensive evaluation of how different thicknesses influence the mechanical behavior, oxidation resistance, and fatigue life of the superalloy under operational conditions. Fatigue performance, in particular, is a critical consideration, as components often undergo cyclic loading at elevated temperatures, which can exacerbate the initiation and propagation of cracks [13]. The interplay between the coating thickness, the diffusion of elements within the superalloy, and the formation of thermally grown oxide (TGO) layers can significantly affect the initiation and growth of fatigue cracks [14]. Thus, a systematic investigation of aluminide coatings with varying thicknesses can provide valuable insights into optimizing coating parameters for enhanced high-temperature performance. A thicker coating generally offers better protection against oxidative and corrosive environments, as it acts as a more substantial barrier to external aggressive species, reducing the rate of degradation of the substrate [15]. However, excessively thick coatings can have detrimental effects on the fatigue life of nickel-based superalloys. Thick coatings may introduce significant stress concentrations at the interface due to thermal mismatch and differential thermal expansion between the coating and the substrate, especially during thermal cycling, which is common in high-temperature applications [16]. This mismatch can lead to the development of interfacial cracks or delamination, which act as sites for crack initiation, adversely affecting fatigue performance [17]. Conversely, thinner coatings may not provide adequate protection against environmental factors, resulting in surface oxidation, corrosion, and the eventual degradation of fatigue properties due to surface-initiated cracks. Ideally, the coating thickness should be optimized to balance between providing sufficient environmental protection and minimizing adverse mechanical effects.

Previous studies, summarized in review paper [4], have primarily focused on the fundamental aspects of aluminide coatings and their general benefits in protecting superalloys. However, a detailed investigation into the specific influence of coating thickness on the high-temperature behavior of MAR-M247 remains limited. In particular, the relationship between coating thickness, fatigue behavior, and microstructural stability at elevated temperatures requires further exploration. Understanding the interaction between the coating and the underlying superalloy during service conditions is crucial for predicting long-term performance and reliability.

This study aims to address these gaps by systematically evaluating the high-temperature performance of MAR-M247 with aluminide coatings of varying thicknesses. Through a combination of experimental fatigue testing and microstructural analysis, this research seeks to elucidate the effects of coating thickness on the mechanical properties and durability of the superalloy at elevated temperatures. The findings are expected to contribute to the optimization of coating strategies for MAR-M247 and similar nickel-based superalloys, ultimately leading to improved performance and the longevity of critical components in high-temperature applications. By providing a deeper understanding of the role of aluminide coating thickness, this research will support the design and engineering of advanced materials capable of meeting the stringent demands of the modern aerospace and energy industries.

2. Materials and Methods

2.1. Material and Coating Deposition

In this paper, casted, coarse-grained MAR-M247 with the chemical composition presented in Table 1 was used. In order to further enhance its high-temperature performance, the CVD process was performed using optimized parameters [2] (Table 2). The specimen surface was machined before deposition. Coatings were deposited using a low-activity aluminum process on Ion-Bond setup (Ion Bond Bernex BPX Pro 325 S, IHI Ion bond AG, Olten, Switzerland). There was no additional heat treatment, as the deposition temperature of 1040 °C falls within a range suitable for solution heat treatment.

Table 1. Chemical composition of MAR-M247.

C	Cr	Mn	Si	W	Co	Al	Ni
0.09	8.80	0.10	0.25	9.70	9.50	5.70	Bal.

Table 2. CVD process parameters [2].

Coating Thickness	Deposition Time	Deposition Temperature	Internal Pressure	Protective Atmosphere
20 µm	4 h	1040 °C	150 mbar	Hydrogen
40 µm	12 h			

2.2. Experimental Testing

High-temperature fatigue testing was performed at 900 °C using an MTS 810 testing machine (MTS System, Eden Prairie, MN, USA) equipped with a high-temperature MTS extensometer (Figure 1a,b). Fatigue tests were force-controlled under a zero-mean-value, constant stress amplitude with a frequency of 20 Hz in the stress amplitude range from 400 MPa to 520 MPa. The geometry of the specimens is presented in Figure 1c. Temperature stability was monitored and controlled using a bicolor infrared pyrometer (Fluke Process Instruments, Everett, WA, USA). Cyclic loading was initiated after 0.5 h once the testing temperature was reached. During this time, the testing machine was operated with force control to maintain a force near 0 kN in order to reduce the thermal expansion effects on the material's behavior during testing. The microstructural characterization and chemical composition analysis were undertaken on grounded and mechanically polished cross-sections of coated specimens using a Hitachi 2600 N scanning electron microscope with an Energy-Dispersive Spectroscopy (EDS) attachment (Oxford Instruments, Oxford, UK). The coating's phase composition was analyzed by the grazing incidence X-ray diffraction (GI XRD) technique based on Co K α 1 radiation ($\lambda = 1.78892 \text{ \AA}$), using a Rigaku Ultima IV system with a parallel beam mode of radiation.

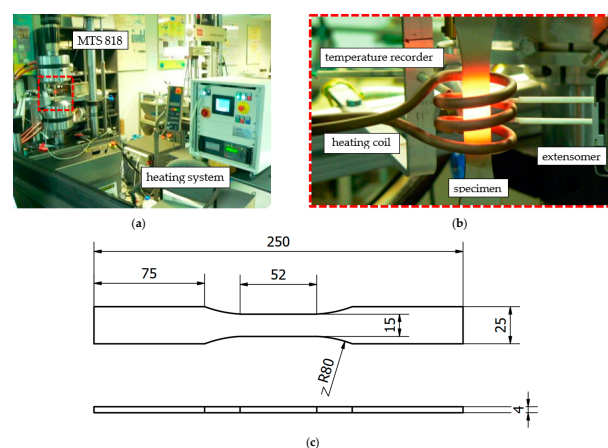


Figure 1. (a) General view of the experimental setup; (b) enlarged view of the heated specimen during high-temperature fatigue testing; (c) engineering drawing of the specimen.

3. Results and Discussion

3.1. Microstructural Characterization of the As-Received Material and Deposited Aluminide Coatings

MAR-M247 was characterized by a coarse microstructure with equiaxed grains, as presented in Figure 2. It is mainly composed of a gamma-phase, face-centered cubic (FCC) structure, which acts as a matrix for the distribution of strengthening phases and provides the alloy with ductility and toughness. It is usually solid-solution-strengthened by elements like Co, Cr, Mo, W, and Nb. In the matrix, one can find gamma prime precipitates, such as $\text{Ni}_3(\text{Al,Ti})$, and an ordered L122 structure, where Ni atoms occupy the face-centered positions and Al or Ti atoms are at the corners of the unit cell [18]. The γ' phase is primarily responsible for the high-temperature strength of MAR-M247, impeding dislocation motion and thereby increasing creep resistance.

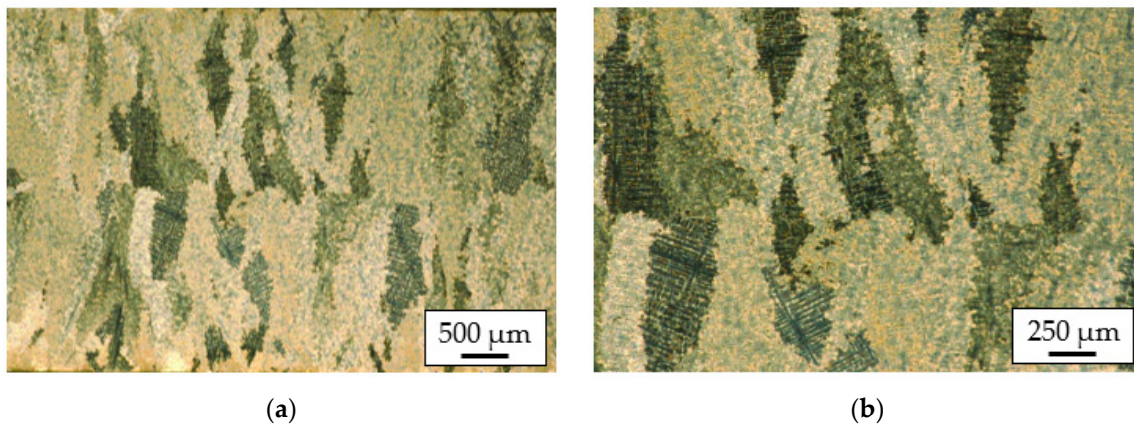


Figure 2. Microstructure of MAR-M247 under different magnifications: (a) 500 \times ; (b) 1000 \times .

Depending on the deposition time, coatings of 20 μm and 40 μm in thickness were obtained after 4 h and 12 h, respectively (Figure 3). Both exhibited a two-layer structure consisting of an outer layer (β -NiAl) rich in aluminum, providing excellent oxidation resistance, and an inner diffusion zone ($\gamma' + \beta$) with a mixture of γ' (Ni_3Al) and β -NiAl phases, offering a transition zone adhering strongly to the substrate [4]. The outer layer, composed mainly of β -NiAl, provides a continuous aluminum oxide film, and is responsible for oxidation resistance [19]. In the interlayer zone, aluminum diffuses into the base alloy, forming a gradient that ensures strong adhesion and minimizes thermal expansion mismatches. One should mention that the CVD process leads to interdiffusion between the coating and the substrate, creating a metallurgical bond that enhances mechanical stability [20].

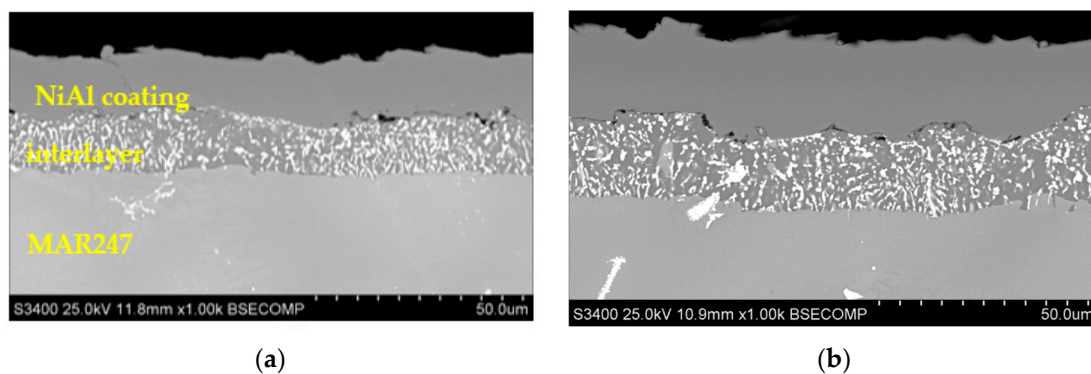


Figure 3. Cross-sectional view of MAR-M247 with different coating thicknesses deposited: (a) 20 μm ; (b) 40 μm .

Based on Figure 3, one can conclude that deposition time significantly influences the composition and structure of aluminide coatings on MAR-M247, particularly in the formation of the outer β -NiAl layer and the inner diffusion zone ($\gamma' + \beta$). During aluminizing, an extended deposition time allows more aluminum to diffuse into the substrate, promoting the growth of a thicker β -NiAl outer layer, which is crucial for oxidation resistance [2]. Simultaneously, prolonged deposition enhances the inward diffusion of aluminum and the outward diffusion of nickel, leading to a more pronounced and thicker diffusion zone where phases like γ' (Ni_3Al) and β (NiAl) coexist [2]. This diffusion zone, enriched with aluminum and characterized by the $\gamma' + \beta$ structure, plays a critical role in accommodating thermal stresses and enhancing the mechanical stability of the coating. However, excessively long deposition times can result in overly thick coatings, which may introduce brittleness or cause unwanted phase transformations, potentially compromising the coating's overall performance.

Based on EDS maps (Figure 4), one can observe that the concentration of aluminum gradually decreases from the outer aluminide layer to the IDZ. This gradient is essential for maintaining the protective oxide layer and facilitating the adherence of the coating to the substrate [21]. Nickel concentration increases towards the IDZ. This region often consists of mixed phases like γ -Ni and β -NiAl, forming a transition zone that enhances mechanical bonding [22]. Chromium concentration is also notable in the IDZ, originating from the MAR-M247 substrate. The element distribution in aluminide coatings on MAR-M247 is governed by diffusion mechanisms, thermal processing, and the interaction between the coating and the substrate materials. Aluminum diffuses inward from the coating, forming a gradient that is essential for oxidation resistance [23]. This diffusion results in a transition from high aluminum content in the outer layer to lower content in the IDZ. The gradient of aluminum concentration from the outer aluminide layer to the interdiffusion zone is crucial for both maintaining the protective oxide layer and ensuring strong adherence of the coating to the substrate. In the outer aluminide layer, where the aluminum concentration is highest, a dense and continuous aluminum oxide (Al_2O_3) layer forms when exposed to high temperatures [24]. This oxide layer acts as a barrier, preventing further oxidation of the underlying material. As the aluminum content gradually decreases toward the interdiffusion zone, the phase composition transitions, providing a buffer that accommodates thermal and mechanical stresses between the brittle outer β -NiAl layer and the more ductile nickel-based superalloy substrate [25]. This gradient in aluminum concentration helps to prevent the formation of cracks and delamination, which could compromise the coating's protective properties. Additionally, the interdiffusion zone, with its mix of γ' (Ni_3Al) and β (NiAl) phases, ensures that the coating remains firmly anchored to the substrate, enhancing the overall durability and effectiveness of the oxidation resistance [25]. Nickel and elements from the substrate (such as chromium, cobalt, tungsten, tantalum, and titanium) diffuse outward into the coating. This outward diffusion forms the interdiffusion zone, which stabilizes the microstructure and enhances adhesion [26]. The interaction between diffusing elements leads to the formation of intermetallic phases, such as γ' - Ni_3Al , M_xC carbides, and other complex phases in the IDZ. These phases provide structural stability and mechanical strength.

The XRD graph of the aluminide coating on MAR-M247 prominently features peaks indicative of the β -NiAl phase, which is crucial for oxidation resistance and mechanical stability at high temperatures (Figure 5). This phase typically exhibits distinctive peaks at 2θ angles around 20.7° (110), 29.4° (200), 43.6° (211), and 63.0° (220), corresponding to its B2 cubic crystal structure. The 110 peak is usually the most intense, reflecting the high concentration and well-ordered nature of the β -NiAl phase within the coating, which serves as the primary barrier against oxidation. These sharp peaks indicate a predominantly crystalline structure with few defects. The presence of such well-defined peaks for β -NiAl confirms the effective formation of the aluminide layer, which is critical for maintaining the structural integrity and oxidation resistance of the underlying MAR-M247 substrate.

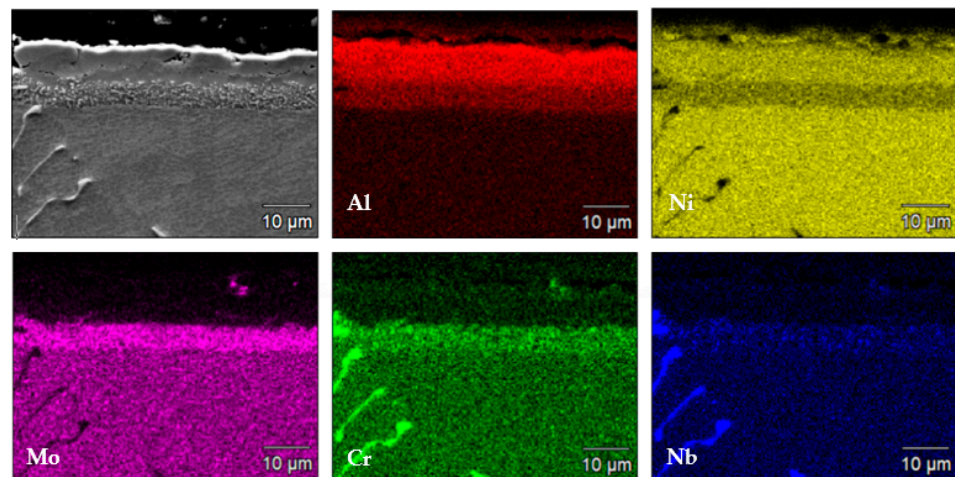


Figure 4. EDS maps showing the distribution of specific elements.

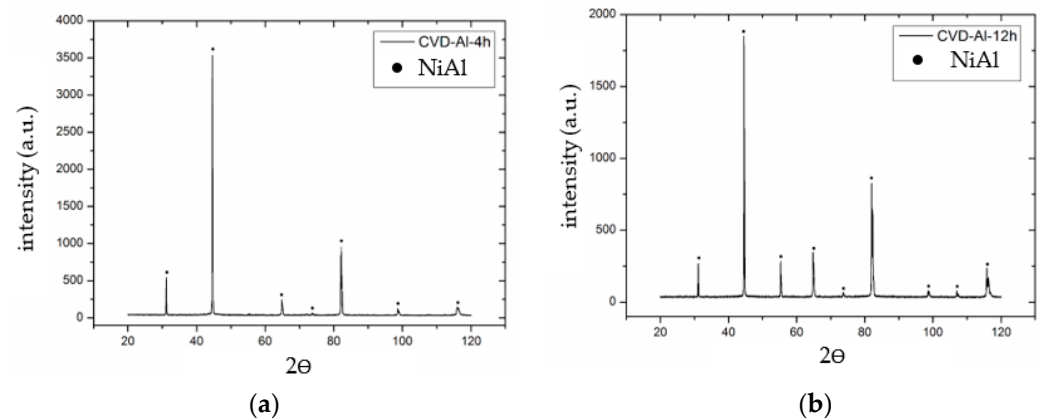


Figure 5. XRD phase analysis of coatings considering deposition time and corresponding coating thickness: (a) 4 h–20 μm ; (b) 12 h–40 μm .

3.2. High-Temperature Fatigue Testing

The S-N curves for MAR-M247 with different coating thicknesses are presented in Figure 6a. It can be observed that no significant effect of coating thickness was found since the material exhibited a similar service life throughout the fatigue test when subjected to the same stress amplitude. An enhanced service life of the 40 μm coating was observed for stress amplitudes equal to 450 MPa and 400 MPa; however, the differences were relatively small. In order to compare the fatigue performance of NiAl-coated MAR-M247, the hysteresis loops for different coating thicknesses and stress amplitudes were compared (Figure 6b–e). For each condition, the first cycle, midlife performance, and last cycle were investigated. It was found that the material's behavior was reflected in the ratcheting effect, characterized by a progressive, incremental inelastic deformation leading to a shift in the stress–strain hysteresis loop along the strain axis [27]. The width of the hysteresis loop observed for MAR-M247 with 20 μm NiAl slightly increased in the following cycles (Figure 6b), suggesting the occurrence of a cyclic plasticity effect [28]. Such behavior was, however, not observed for MAR-M247 with 40 μm NiAl subjected to the same stress amplitude equal to 400 MPa (Figure 6d). For this coating, the width of the hysteresis loop remained almost constant, which may be attributed to the higher stiffness of the thicker coating. The high-temperature fatigue testing at a stress amplitude of 500 MPa did not expose significant differences, except for the higher strain accumulation in MAR-M247 with the 20 μm NiAl coating reflected by the shift of the hysteresis loop.

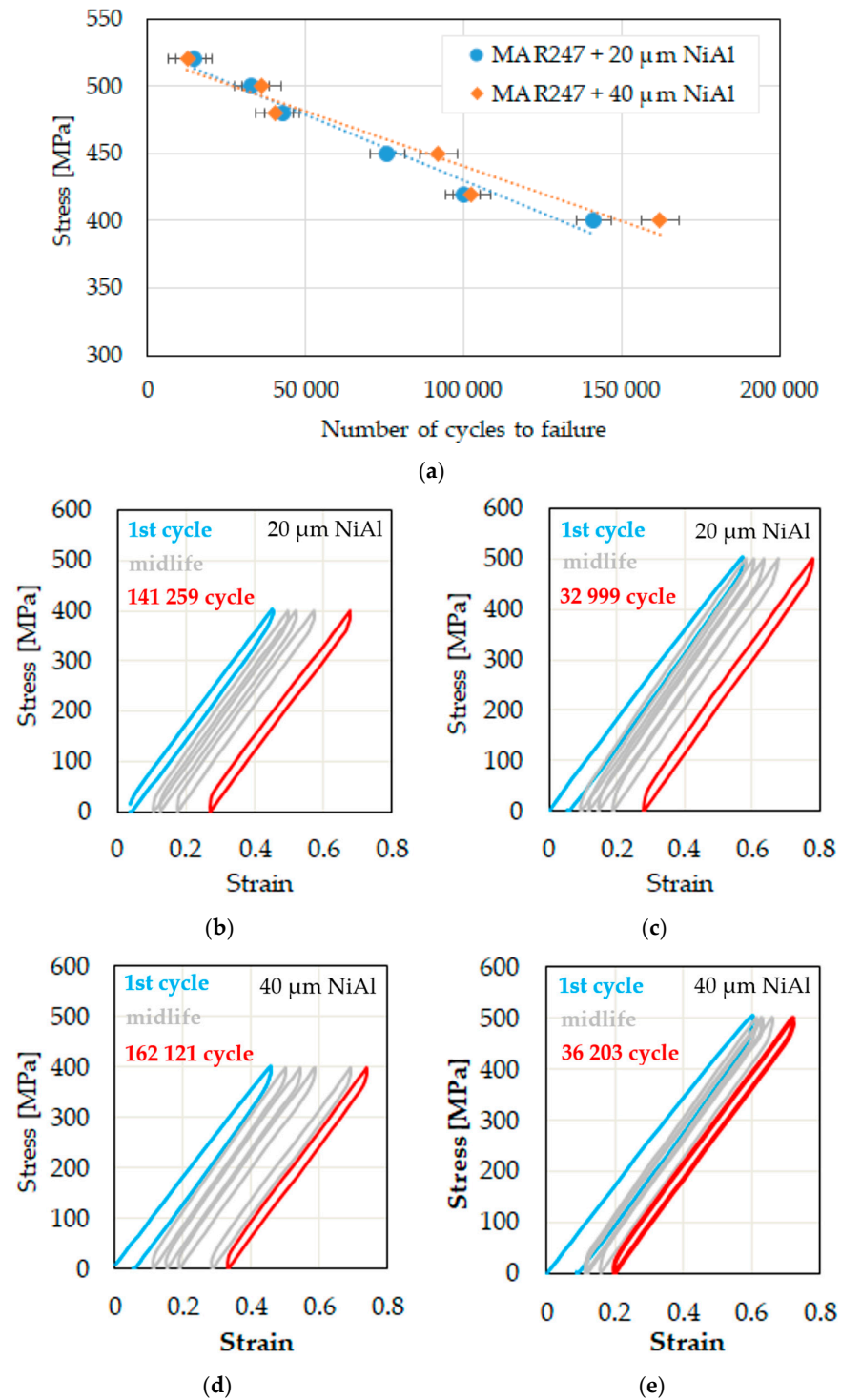


Figure 6. (a) S-N curves for MAR-M247 with different coating thicknesses; hysteresis loops for coating thicknesses of 20 μm (b,c) and 40 μm (d,e) subjected to fatigue testing at stress amplitudes of 400 MPa and 500 MPa, respectively.

The high-temperature fatigue performance of nickel-based superalloys with thermal barrier coatings (TBCs) is a critical area of study in the aerospace and power-generation industries due to the need for materials that can withstand extreme operating environments while maintaining structural integrity and reliability. Nickel-based superalloys, such as Inconel 718, René 88, and CMSX-4, are known for their exceptional mechanical properties, including high strength, creep resistance, and oxidation resistance at elevated tempera-

tures. However, when subjected to high-temperature fatigue conditions, these alloys can experience significant degradation mechanisms that impact their long-term performance. Therefore, TBCs are applied to protect the superalloy substrate from thermal stresses and oxidative environments. These coatings play a crucial role in enhancing fatigue life by reducing the thermal gradient and decreasing the metal temperature, thereby mitigating the effects of thermal cycling. Bortoluci et al. [29] presented that the CMSX-4 Plus alloy with a NiAl coating exhibited improved fatigue life as compared to the AM1, CMSX-4, and Rene N5 alloys at 1000 °C. Barwinska et al. [5] reported improved fatigue performance and oxidation resistance at 1000 °C in air for Inconel 740 with a NiAl coating. Sulak et al. [8] found that Inconel 713LC with a NiAl coating was characterized by enhanced low-cycle fatigue behavior at 800 °C. One should note that the application of TBCs also introduces new challenges, as the bond coat can experience phase transformations, oxidation, and interfacial degradation, which may act as crack-initiation sites under cyclic loading [30]. The fatigue performance of these coated systems is largely governed by the microstructural stability of both the superalloy and the coating system, where factors such as grain boundary strengthening, phase stability, and resistance to oxidation at high temperatures are critical [31]. Additionally, the mismatch in thermal expansion coefficients between the ceramic topcoat and the metallic substrate can induce residual stresses, leading to coating delamination or spallation under fatigue conditions [32].

3.3. Fractographic Observations

The observations on the fracture surfaces of the tested specimens after the high-temperature fatigue test showed no effect of coating thickness on fracture mode (Figures 7 and 8). One should stress that the coating remained well adhered after specimen fracture (Figures 7a and 8a), confirming its effectiveness in protecting the material against high-temperature oxidation. Thus, the fracture mechanisms were mainly associated with the performance of MAR-M27, which exhibits a complex and intricate array of features that reflect the alloy's response to cyclic thermal and mechanical stresses. The fracture surfaces revealed a combination of oxidation-assisted damage (Figures 7a and 8a), intergranular cracking (Figures 7b and 8b), fatigue striations (Figures 7c and 8), and areas of both ductile and brittle fracture (Figures 7c and 8). Fatigue striations are prominent on fracture surfaces and are characterized by regularly spaced, parallel lines that form perpendicular to the crack propagation direction, indicating the progressive nature of fatigue crack growth with each loading cycle. Intergranular cracking is another significant feature, particularly prevalent in MAR-M247 at high temperatures, where cracks propagate along grain boundaries due to a combination of oxidation-induced embrittlement and the presence of brittle phases. This intergranular failure is often exacerbated by the oxidation of grain boundary carbides, such as MC-type carbides (primarily tantalum carbides), leading to weakened interfaces and facilitating crack growth along these paths [33]. Additionally, transgranular cracking can be observed, characterized by crack propagation through the grains, which is typically associated with regions of high stress concentration or where the γ' precipitates have coarsened or transformed into less stable phases under thermal exposure, reducing their strengthening capability [34]. The fracture surfaces may also exhibit ductile dimple features, especially in areas of final overload, where the material undergoes localized plastic deformation before ultimate failure. These dimples are indicative of microvoid coalescence, where voids nucleate, grow, and merge under tensile loading, providing evidence of the alloy's ability to deform plastically despite challenging conditions. In contrast, regions of brittle fracture display cleavage facets or the failure of gamma prime (γ') and gamma (γ) matrix interfaces, particularly if topologically close-packed (TCP) phases like sigma or Laves phases form, which can embrittle the alloy and contribute to sudden fracture. The presence of oxidation products such as alumina (Al_2O_3) scales is another crucial aspect of fracture surfaces, often concentrated around crack-initiation sites or along crack paths. These oxidation products indicate the role of high-temperature oxidation in accelerating fatigue crack growth by causing localized embrittlement or by creating stress concentrations

at the oxide–metal interface. The oxidation of nickel-based alloys results in the development of a protective external layer of chromia, accompanied by the formation of alumina beneath the surface, occurring both intergranularly and intragranularly [35]. Beneath this layer lies a region that is weaker due to a depletion of γ' particles (typically $\text{Ni}_3(\text{Al,Ti})$) and grain-boundary carbides (commonly M_{23}C_6). The emergence of these internal oxides within the subsurface is unfavorable and can significantly impair the mechanical properties of nickel-based superalloys. These internal oxides formed at the grain boundaries may be prone to cracking, leading to localized stress concentrations that facilitate early failure, thereby diminishing the lifespan of the components [35].

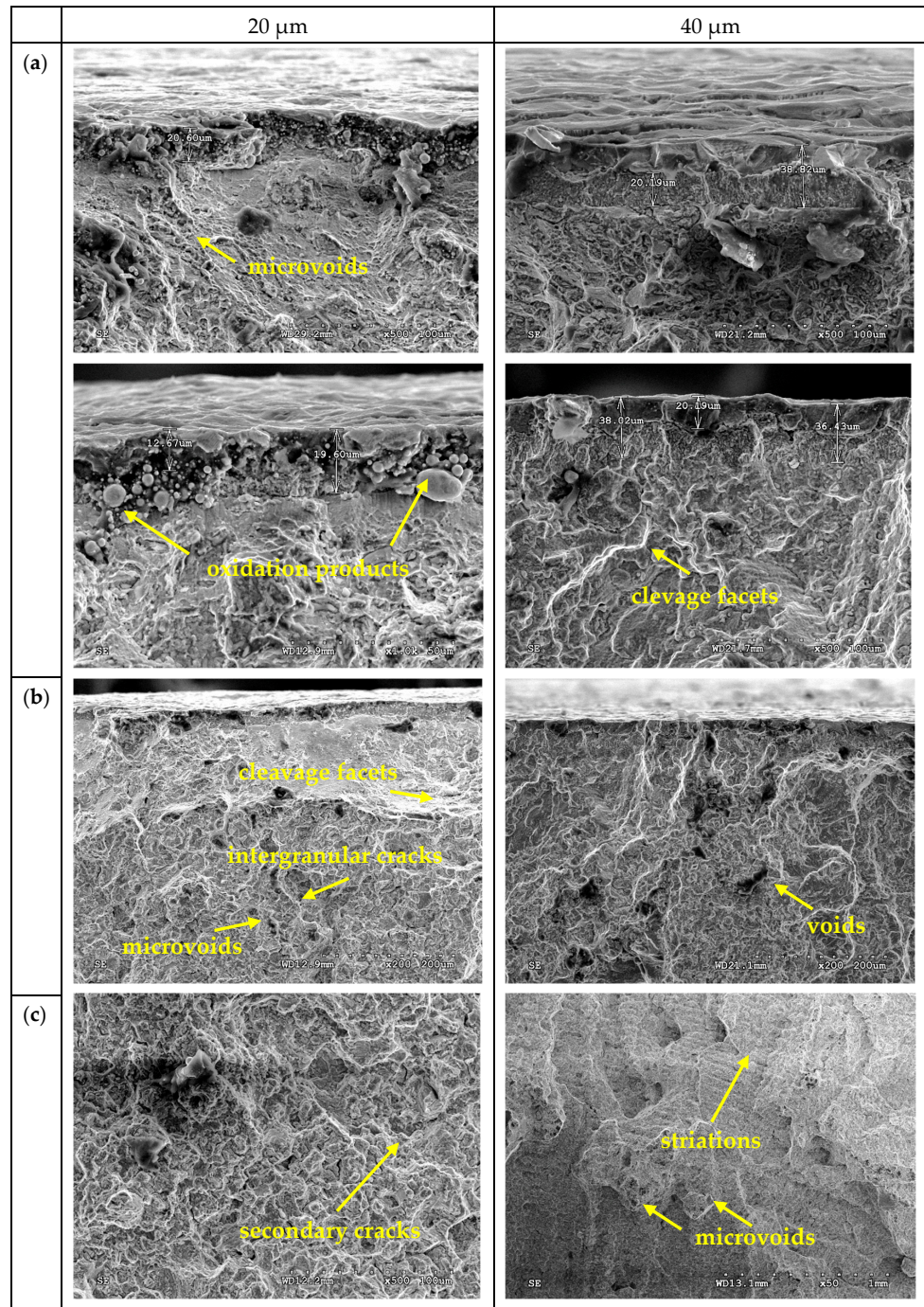


Figure 7. Fracture surfaces of MAR-M247 with NiAl coating after fatigue testing at stress amplitude equal to 400 Mpa. Three views: (a) detailed and (b) general sub-surface structure; (c) fractured view of the middle part of the specimen.

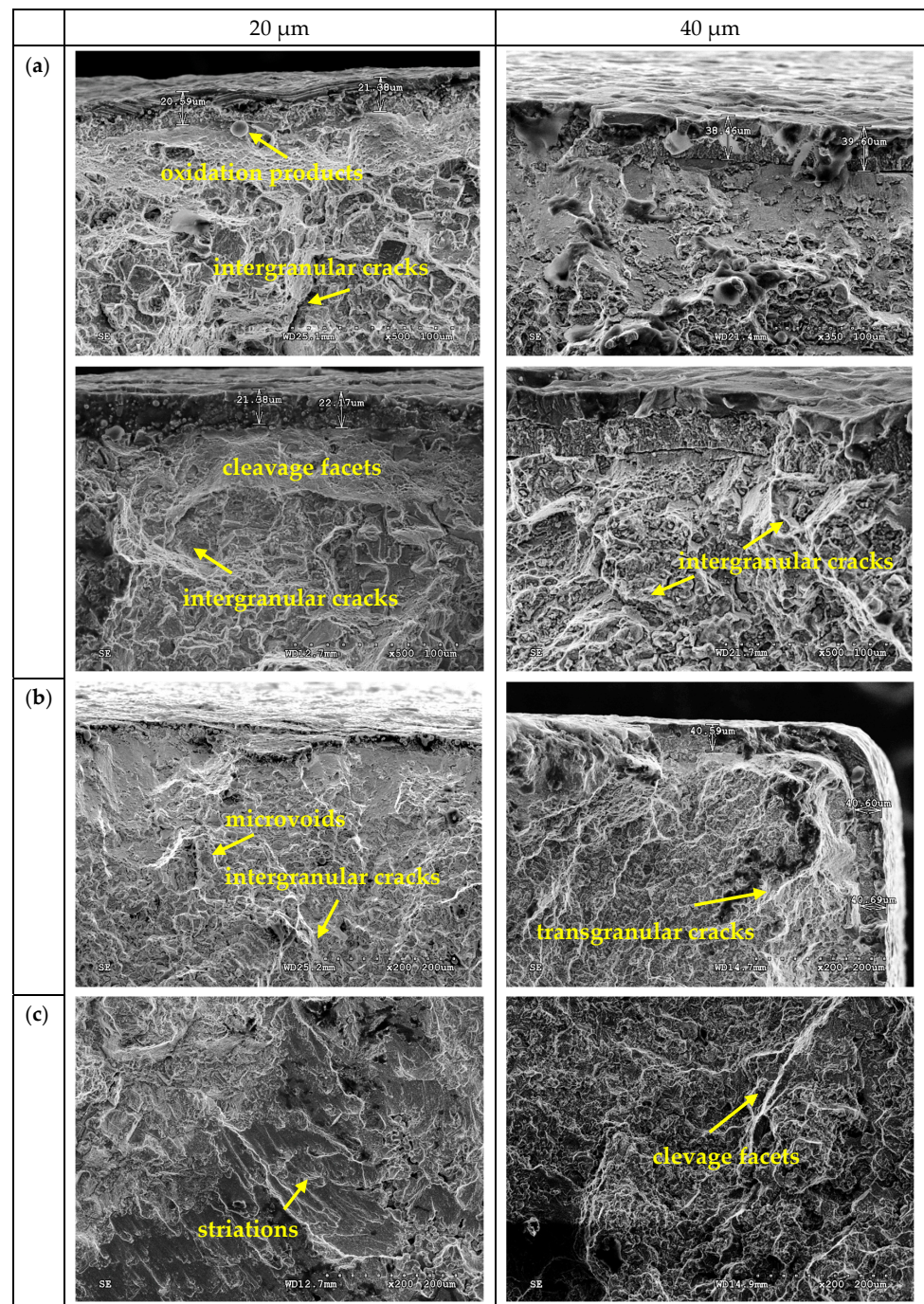


Figure 8. Fracture surfaces of MAR-M247 with NiAl coating after fatigue testing at stress amplitude equal to 500 MPa. Three views: (a) detailed and (b) general sub-surface structure; (c) fractured view of the middle part of the specimen.

4. Conclusions

In this paper, the effect of aluminide coating thickness (20 μm and 40 μm) on the high-temperature performance of an MAR-M247 nickel-based superalloy was examined during a fatigue test at 900 $^{\circ}\text{C}$. MAR-M247 with two coating thicknesses exhibited a similar service life throughout the fatigue test cycles when subjected to the same stress amplitude. The fracture surfaces reveal a combination of oxidation-assisted damage, intergranular cracking, fatigue striations, and areas of both ductile and brittle fracture. Although no significant differences in service life for either thickness were found, both remained well adhered to the specimen after its fracture. Such behavior confirms the coating's effectiveness in

protecting the material against high-temperature oxidation. Therefore, the optimized CVD process performed in a hydrogen protective atmosphere for 4 h and 12 h at a temperature of 1040 °C and an internal pressure of 150 mbar could be successfully used for real-size components to protect them against oxidation at high temperature. Furthermore, it is suggested that coatings of lower thickness should be applied in order to reduce the cost of the CVD process by limiting the coating deposition time to 4 h.

Funding: This research received no external funding.

Institutional Review Board Statement: Not applicable.

Informed Consent Statement: Not applicable.

Data Availability Statement: Data are contained within the article.

Acknowledgments: The author is grateful to Mirosław Wyszowski and Dominik Kukla for their help during the experimental part of this work.

Conflicts of Interest: The author declares no conflicts of interest.

References

1. Barwinska, I.; Kopec, M.; Kukla, D.; Senderowski, C.; Kowalewski, Z.L. Thermal Barrier Coatings for High-Temperature Performance of Nickel-Based Superalloys: A Synthetic Review. *Coatings* **2023**, *13*, 769. [\[CrossRef\]](#)
2. Kukla, D.; Kopec, M.; Kowalewski, Z.L.; Politis, D.J.; Jóźwiak, S.; Senderowski, C. Thermal Barrier Stability and Wear Behavior of CVD Deposited Aluminide Coatings for MAR 247 Nickel Superalloy. *Materials* **2020**, *13*, 3863. [\[CrossRef\]](#) [\[PubMed\]](#)
3. Šmíd, M.; Kunz, L.; Hutař, P.; Hrbáček, K. High Cycle Fatigue of Nickel-based Superalloy MAR-M 247 at High Temperatures. *Procedia Eng.* **2014**, *74*, 329–332. [\[CrossRef\]](#)
4. Kopec, M. Recent Advances in the Deposition of Aluminide Coatings on Nickel-Based Superalloys: A Synthetic Review (2019–2023). *Coatings* **2024**, *14*, 630. [\[CrossRef\]](#)
5. Barwinska, I.; Kopec, M.; Kukla, D.; Łazińska, M.; Sitek, R.; Kowalewski, Z.L. Effect of Aluminizing on the Fatigue and High-Temperature Corrosion Resistance of Inconel 740 Nickel Alloy. *JOM* **2023**, *75*, 1482–1494. [\[CrossRef\]](#)
6. Morgiel, J.; Dudziak, T.; Rząd, E.; Morgiel, K.; Kateusz, F. Morphology and microstructure of Yb₂O₃ layer formed over aluminide coating produced by pack cementation of Haynes[®] 263 alloy. *Archiv. Civ. Mech. Eng.* **2024**, *24*, 59. [\[CrossRef\]](#)
7. Nourpoor, P.; Javadian, S.; Aghdam, A.S.R.; Ghadami, F. Microstructure Investigation and Cyclic Oxidation Resistance of Ce-Si-Modified Aluminide Coating Deposited by Pack Cementation on Inconel 738LC. *Coatings* **2022**, *12*, 1491. [\[CrossRef\]](#)
8. Sulak, I.; Obrtlík, K.; Hutarova, S.; Julis, M.; Podrabsky, T.; Celko, L. Low cycle fatigue and dwell-fatigue of diffusion coated superalloy Inconel 713LC at 800 °C. *Mater. Charact.* **2020**, *169*, 110599. [\[CrossRef\]](#)
9. Grégoire, B.; Bonnet, G.; Pedraza, F. Development of a new slurry coating design for the surface protection of gas turbine components. *Surf. Coat. Technol.* **2019**, *374*, 521–530. [\[CrossRef\]](#)
10. Kepa, T.; Bonnet, G.; Pedraza, F. Oxidation behaviour of ultrafast slurry aluminized nickel. *Surf. Coat. Technol.* **2021**, *424*, 127667. [\[CrossRef\]](#)
11. Brunner, M.; Bensch, M.; Völkl, R.; Affeldt, E.; Glatzel, U. Thickness influence on creep properties for Ni-based superalloy M247LC SX. *Mater. Sci. Eng. A* **2012**, *550*, 254–262. [\[CrossRef\]](#)
12. Busso, E.P.; Evans, H.E.; Qian, Z.Q.; Taylor, M.P. Effects of breakaway oxidation on local stresses in thermal barrier coatings. *Acta Mater.* **2010**, *58*, 1242–1251. [\[CrossRef\]](#)
13. Kedir, Y.A.; Lemu, H.G. Prediction of Fatigue Crack Initiation under Variable Amplitude Loading: Literature Review. *Met* **2023**, *13*, 487. [\[CrossRef\]](#)
14. Wang, P.; Zhao, X.; Yue, Q.; Xia, W.; Ding, Q.; Bei, H.; Gu, Y.; Zhang, Z. Crack Initiation in Ni-Based Single Crystal Superalloy under Low-Cycle Fatigue-Oxidation Conditions. *Met* **2023**, *13*, 1878. [\[CrossRef\]](#)
15. Kianicová, M. *Hypersonic and Supersonic Flight-Advances in Aerodynamics, Materials, and Vehicle Design*; Volkov, K., Ed.; IntechOpen: London, UK, 2023. [\[CrossRef\]](#)
16. Bogdan, M.; Peter, I. A Comprehensive Understanding of Thermal Barrier Coatings (TBCs): Applications, Materials, Coating Design and Failure Mechanisms. *Met* **2024**, *14*, 575. [\[CrossRef\]](#)
17. Forschelen, P.J.J.; Suiker, A.S.J.; van der Sluis, O. Effect of residual stress on the delamination response of film-substrate systems under bending. *Int. J. Solids Struct.* **2016**, *97–98*, 284–299. [\[CrossRef\]](#)
18. Baldan, R.; da Rocha, R.L.P.; Tomasiello, R.B.; Nunes, C.A.; da Silva Costa, A.M.; Barboza, M.J.R.; Coelho, G.C.; Rosenthal, R. Solutioning and Aging of MAR-M247 Nickel-Based Superalloy. *J. Mater. Eng Perform.* **2013**, *22*, 2574–2579. [\[CrossRef\]](#)
19. Zhang, W.L.; Li, S.M.; Fu, L.B.; Li, W.; Sun, J.; Wang, T.G.; Jiang, S.M.; Gong, J.; Sun, C. Preparation and cyclic oxidation resistance of Hf-doped NiAl coating. *Corros. Sci.* **2022**, *195*, 110014. [\[CrossRef\]](#)
20. Texier, D.; Monceau, D.; Hervier, Z.; Andrieu, E. Effect of interdiffusion on mechanical and thermal expansion properties at high temperature of a MCrAlY coated Ni-based superalloy. *Surf. Coat. Technol.* **2016**, *307*, 81–90. [\[CrossRef\]](#)

21. Lu, J.; Dang, Y.; Huang, J.; Zhou, Y.; Yang, Y.; Yan, J.; Yuan, Y.; Gu, Y. Preparation and characterization of slurry aluminide coating on Super304H boiler tube in combination with heat-treatment process. *Surf. Coat. Technol.* **2019**, *370*, 97–105. [[CrossRef](#)]
22. Xiang, Z.D.; Burnell-Gray, J.S.; Datta, P.K. Aluminide coating formation on nickel-base superalloys by pack cementation process. *J. Mater. Sci.* **2001**, *36*, 5673–5682. [[CrossRef](#)]
23. Taghipour, M.; Eslami, A.; Bahrami, A. High temperature oxidation behavior of aluminide coatings applied on HP-MA heat resistant steel using a gas-phase aluminizing process. *Surf. Coat. Technol.* **2022**, *434*, 128181. [[CrossRef](#)]
24. Grüters, J.; Galetz, M. Influence of thermodynamic activities of different masteralloys in pack powder mixtures to produce low activity aluminide coatings on TiAl alloys. *Intermet.* **2015**, *60*, 19–27. [[CrossRef](#)]
25. Bozza, F.; Bolelli, G.; Giolli, C.; Giorgetti, A.; Lusvarghi, L.; Sassatelli, P.; Scrivani, A.; Candeli, A.; Thoma, M. Diffusion mechanisms and microstructure development in pack aluminizing of Ni-based alloys. *Surf. Coat. Technol.* **2014**, *239*, 147–159. [[CrossRef](#)]
26. Galetz, M.C.; Oskay, C.; Madloch, S. Microstructural degradation and interdiffusion behavior of NiAl and Ge-modified NiAl coatings deposited on Alloy 602 CA. *Surf. Coat. Technol.* **2019**, *364*, 211–217. [[CrossRef](#)]
27. Farooq, H.; Cailletaud, G.; Forest, S.; Ryckelynck, D. Crystal plasticity modeling of the cyclic behavior of polycrystalline aggregates under non-symmetric uniaxial loading: Global and local analyses. *Int. J. Plast.* **2020**, *126*, 102619. [[CrossRef](#)]
28. Kopeck, M. The analysis of strain response for as-received and exploited 10H2M power engineering steel subjected to low cycle fatigue in plastic regime. *Int. J. Press. Vessel. Pip.* **2024**, *207*, 105110. [[CrossRef](#)]
29. Ormastroni, L.M.B.; Kepa, T.; Cervellon, A.; Villechaise, P.; Pedraza, F.; Cormier, J. Very high cycle fatigue rupture mode at high temperatures of Ni-based superalloys coated with a slurry aluminide. *Int. J. Fatigue* **2024**, *180*, 108107. [[CrossRef](#)]
30. Wu, L.T.; Xiao, P.; Osada, T.; Lee, K.I.; Bai, M. A prominent driving force for the spallation of thermal barrier coatings: Chemistry dependent phase transformation of the bond. *Coat. Acta Mater.* **2017**, *137*, 22–35. [[CrossRef](#)]
31. Reid, M.; Pomeroy, M.J.; Robinson, J.S. Microstructural instability in coated single crystal superalloys. *J. Mater. Process. Technol.* **2004**, *153–154*, 660–665. [[CrossRef](#)]
32. Zhao, W.; Hu, Z.; Wang, L.; Wang, X.; Wu, Q.; Liu, R. Effect of Top-Coat Thickness and Interface Fluctuation on the Residual Stress in APS-TBCs. *Coatings* **2023**, *13*, 1659. [[CrossRef](#)]
33. Kim, D.; Jiang, R.; Evangelou, A.; Sinclair, I.; Reed, P.A.S. Effects of γ' size and carbide distribution on fatigue crack growth mechanisms at 650 °C in an advanced Ni-based superalloy. *Int. J. Fatigue* **2021**, *145*, 106086. [[CrossRef](#)]
34. Lynch, S. A review of underlying reasons for intergranular cracking for a variety of failure modes and materials and examples of case histories. *Eng. Fail. Anal.* **2019**, *100*, 329–350. [[CrossRef](#)]
35. Cruchley, S.; Li, H.Y.; Evans, H.E.; Bowen, P.; Child, D.J.; Hardy, M.C. The role of oxidation damage in fatigue crack initiation of an advanced Ni-based superalloy. *Int. J. Fatigue* **2015**, *81*, 265–274. [[CrossRef](#)]

Disclaimer/Publisher's Note: The statements, opinions and data contained in all publications are solely those of the individual author(s) and contributor(s) and not of MDPI and/or the editor(s). MDPI and/or the editor(s) disclaim responsibility for any injury to people or property resulting from any ideas, methods, instructions or products referred to in the content.